

Supporting Information

Biofilm microenvironment-responsive one-for-all bactericidal nanoplatform for photothermal-augmented multimodal synergistic therapy of pathogenic bacterial biofilm infection

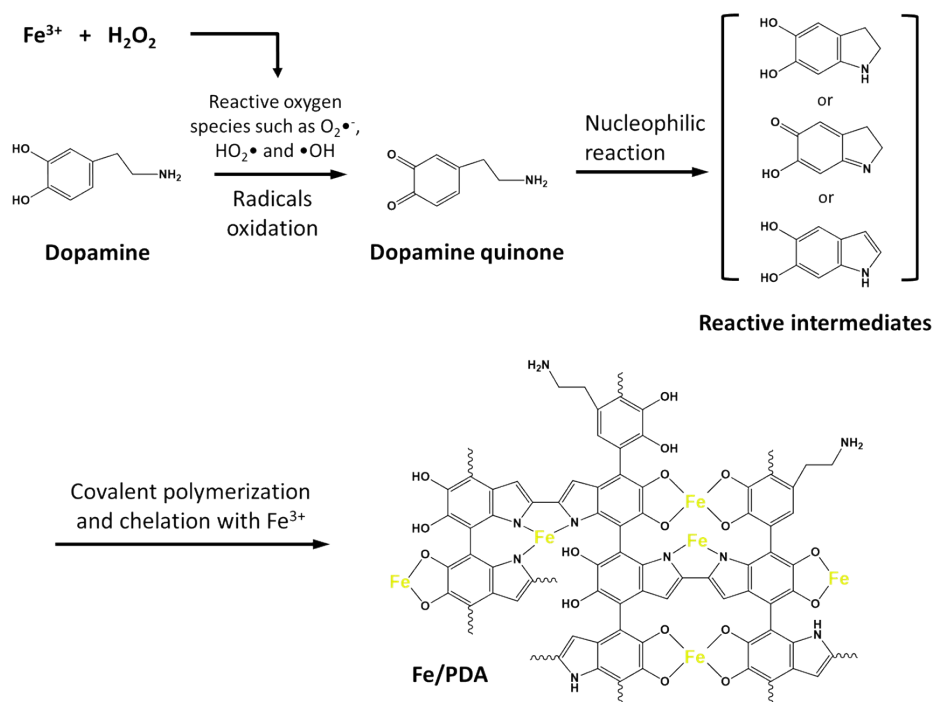
Ke Yang,^{†,a} Luo Hai,^{†,b} Zefeng Wang,^a Huan Li,^a Wenhua Yi,^a Yuze Luo,^a Junqin Li,^a
Le Deng,^{*,a} and Dinggeng He^{*,a}

^aState Key Laboratory of Developmental Biology of Freshwater Fish, College of Life Science, Hunan Normal University, Changsha 410081, China.

^bCentral Laboratory, National Cancer Center/National Clinical Research Center for Cancer/Cancer Hospital & Shenzhen Hospital, Chinese Academic of Medical Sciences & Peking Union Medical College, Shenzhen 518116, China.

[†]These authors contributed equally to this work.

*Corresponding author: hedinggeng@hnu.edu.cn (D. He); dengle@hunnu.edu.cn (L. Deng)



Scheme S1. The proposed mechanism for the formation of Fe^{3+} -doped PDA (Fe/PDA) by using $\text{Fe}^{3+}/\text{H}_2\text{O}_2$ as a trigger.

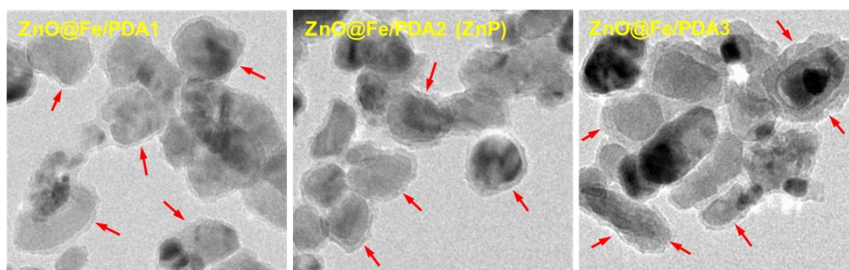


Fig. S1. TEM images of ZnO nanoparticles with different thicknesses of Fe/PDA coating layer. Red arrows indicate the Fe/PDA coating layer.

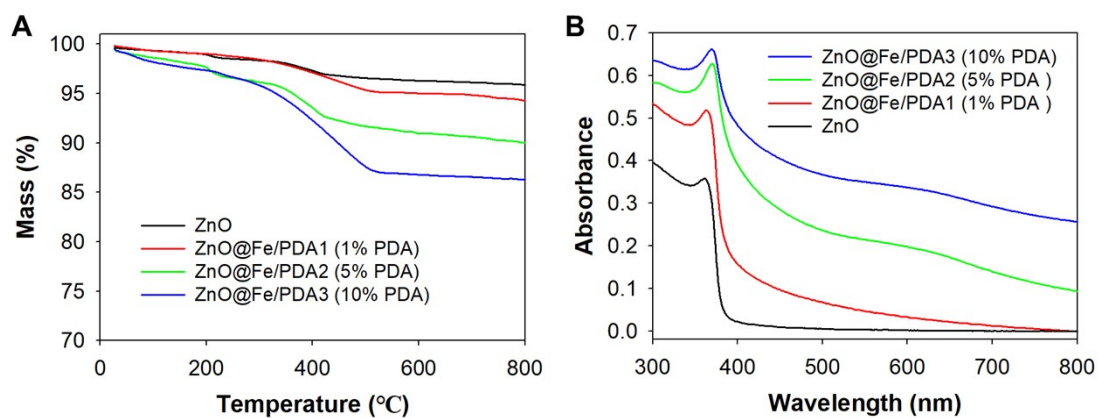


Fig. S2. TGA curves (A) and UV-vis spectra (B) of ZnO nanoparticles without and with different thicknesses of Fe/PDA coating layer.

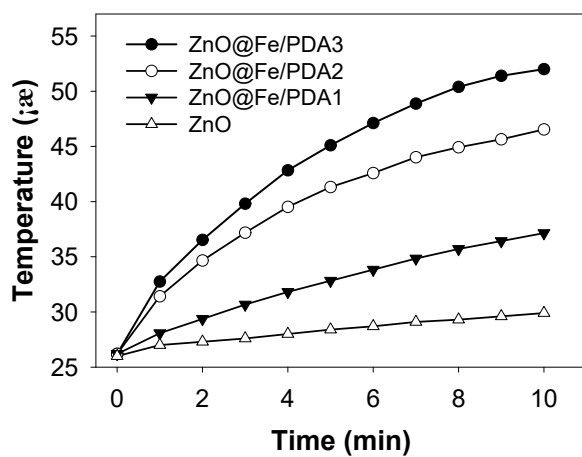


Fig. S3. Photothermal curves of ZnO nanoparticles without and with different thicknesses of Fe/PDA coating layer under 808 nm laser irradiation (1.45 W cm^{-2}) for 10 min.

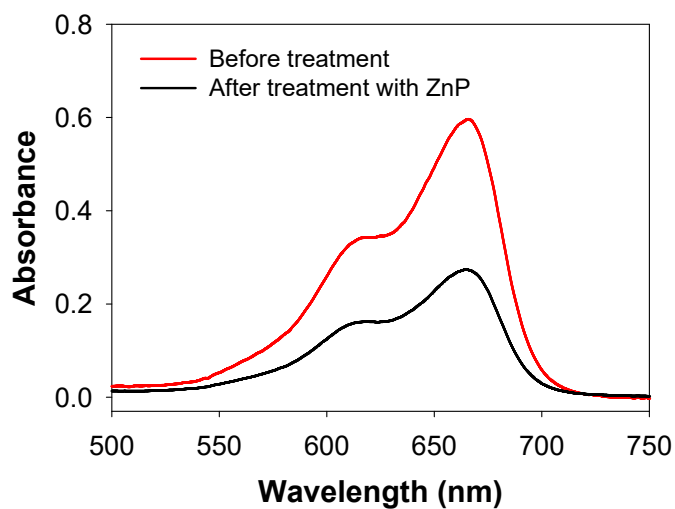


Fig. S4. UV-vis spectra of MB solution before and after treatment with ZnP.

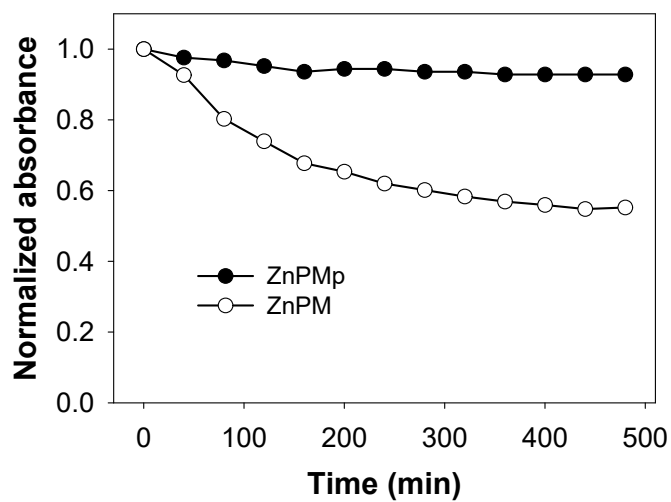


Fig. S5. Stability of MB loaded onto ZnPM and ZnPMp.

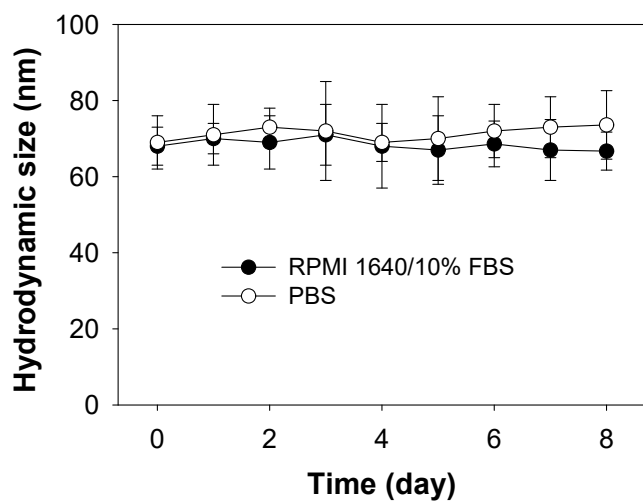


Fig. S6. Long-term stability of ZnPMp in PBS and RPMI 1640 with 10% FBS.

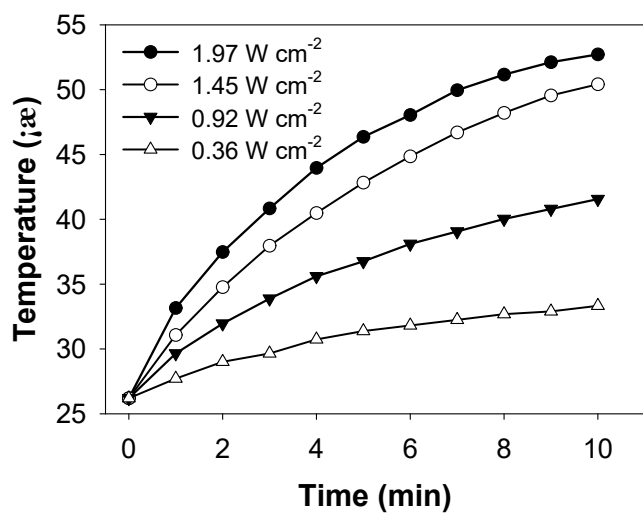


Fig. S7. Photothermal heating curves of ZnPMp ($150 \mu\text{g mL}^{-1}$) receiving irradiation with different laser power densities for 10 min.

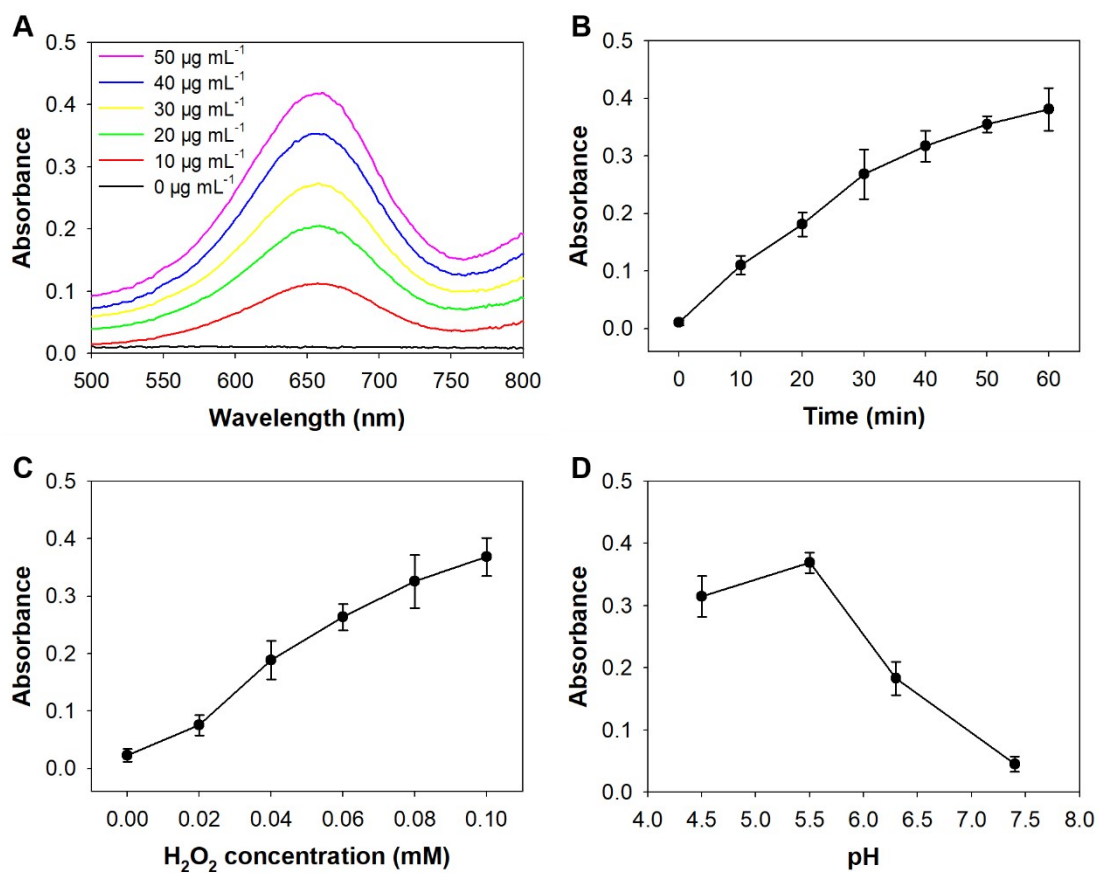


Fig. S10. (A) UV-vis spectra of TMB (10 mM) in the presence of ZnPMp with different concentrations. (B) Time-dependent oxidation of TMB induced by $\bullet\text{OH}$ generation of ZnPMp with 0.1 mM H_2O_2 . (C) UV-vis absorbances of TMB treated with ZnPMp in the presence of different concentrations of H_2O_2 . (D) UV-vis absorbances of TMB co-incubated with ZnPMp at various pH values.

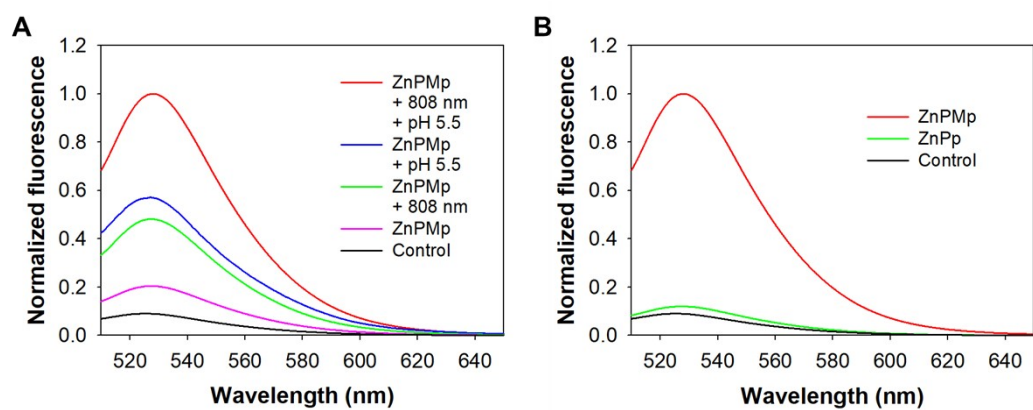


Fig. S11. (A) Normalized SOSG fluorescence of ZnPMp after with different treatments. (B) Normalized fluorescence of ZnPp and ZnPMp with 808 nm laser irradiation at pH 5.5.

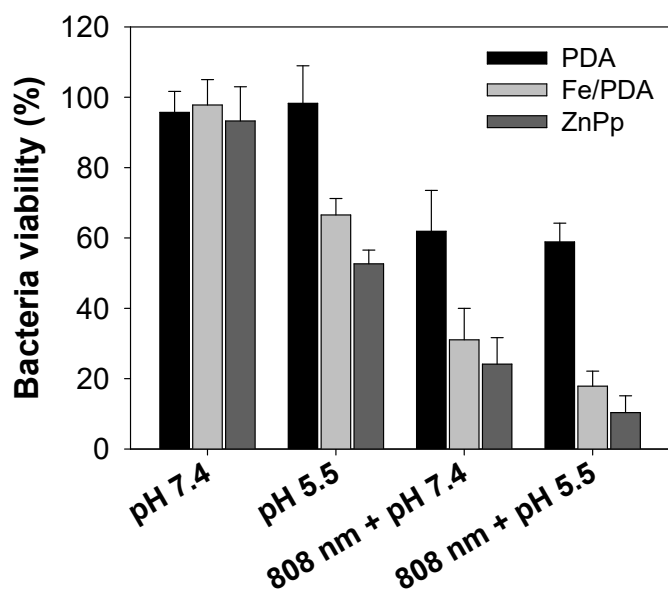


Fig. S12. Viabilities of *S. aureus* with various treatments in the presence of H₂O₂ (0.05 mM).

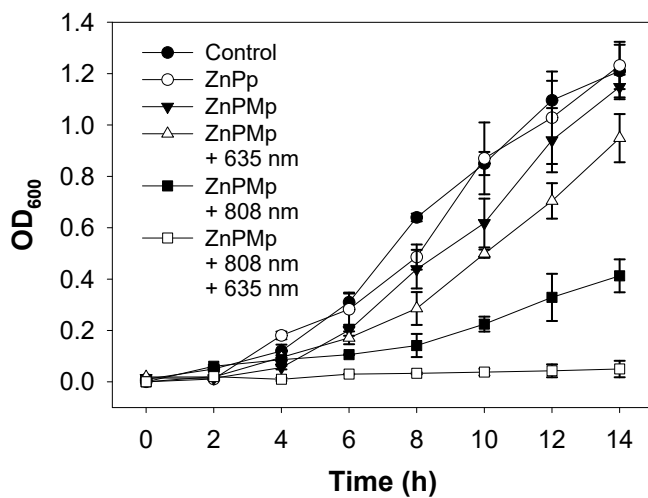


Fig. S13. Growth curves of *S. aureus* with various treatments.

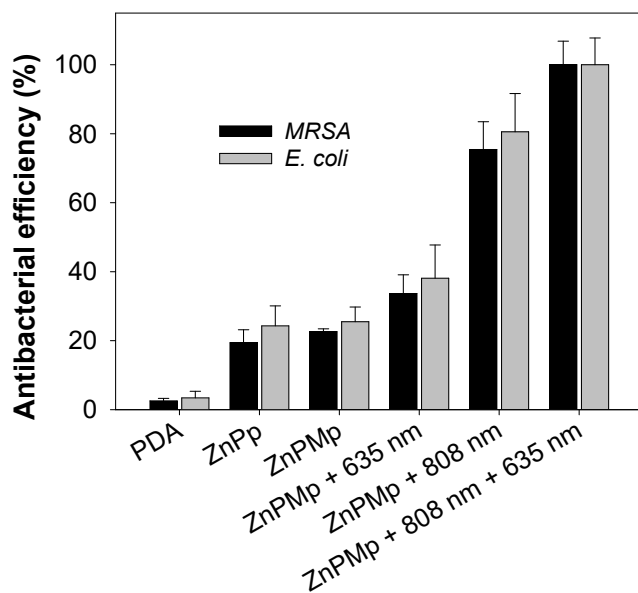


Fig. S14. The antibacterial efficiency of ZnPMp against MRSA and *E. coli* upon exposure to 808 nm and/or 635 nm laser for 10 min or not. The antibacterial effect of PDA and ZnPp on both MRSA and *E. coli* was also showed.

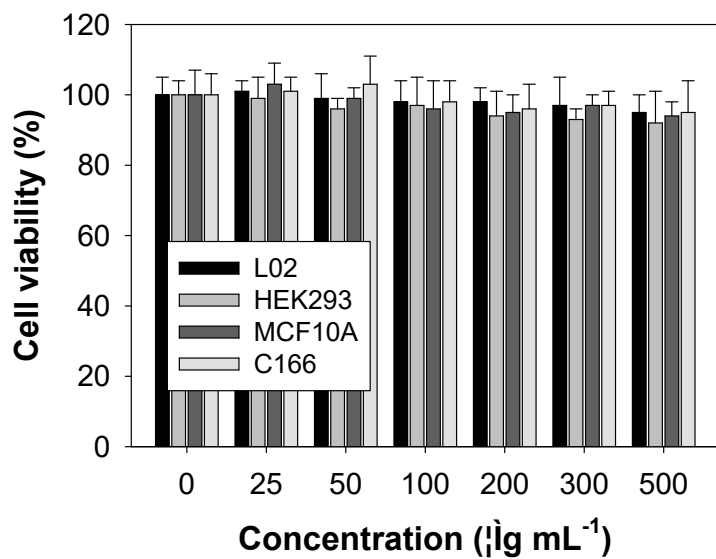


Fig. S15. Viabilities of L02, HEK293, MCF 10A and C166 cells after being treated with ZnPMp (0, 25, 50, 100, 200, 300, and 500 $\mu\text{g mL}^{-1}$) for 48 h.

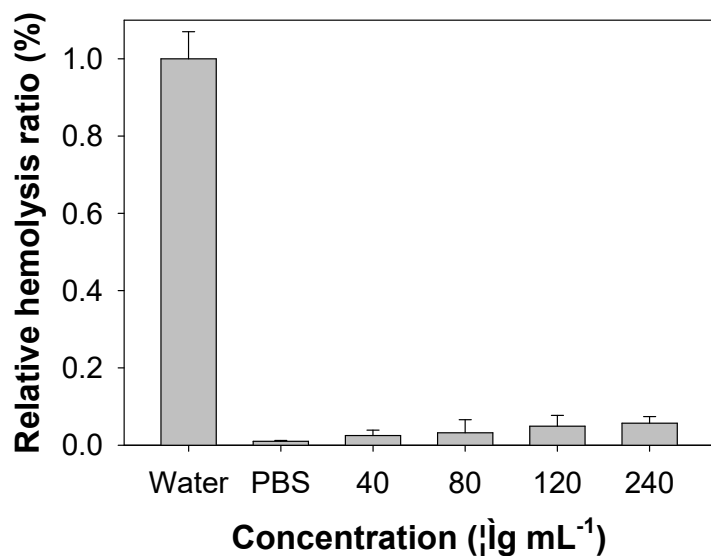


Fig. S16. Relative Hemolysis ratio of red blood cells (RBCs) after incubation with water, PBS and different concentrations of ZnPMp for 4 h.

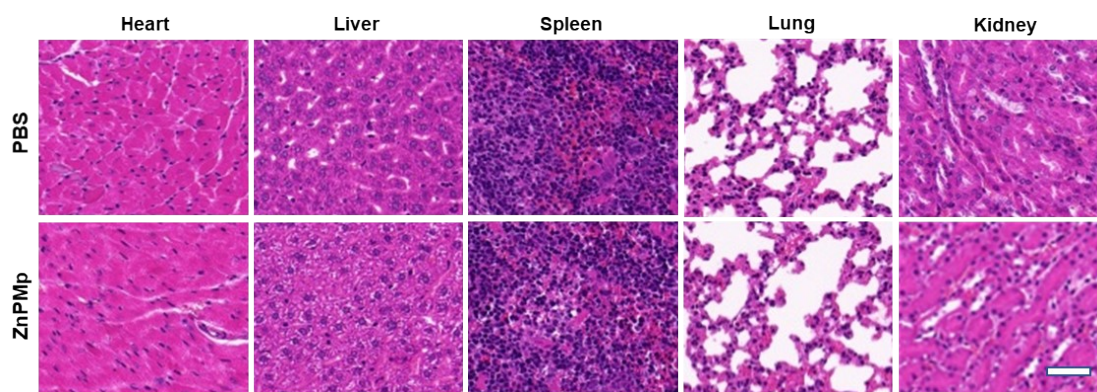


Fig. S17. H&E staining images of major organs (heart, liver, spleen, lung, and kidney) from mice treated with PBS and ZnPMp after 2 weeks. Scale bar: 50 μm .

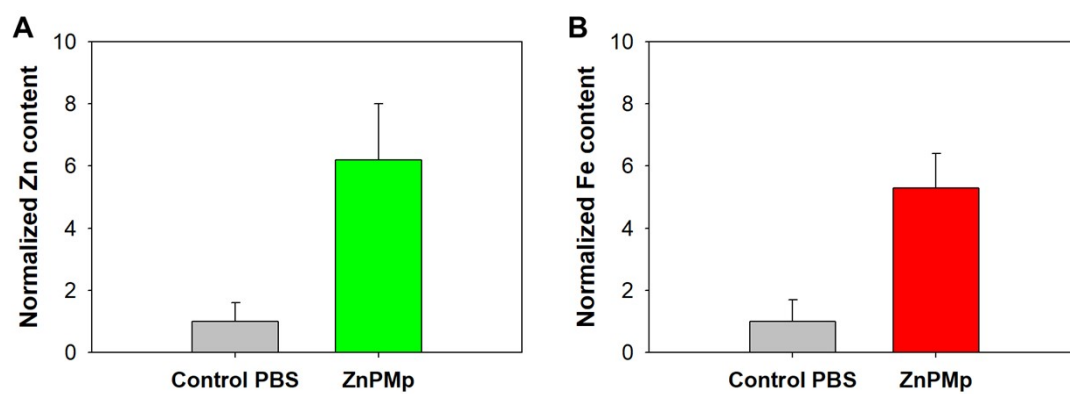


Fig. S18. Normalized Zn (A) and Fe (B) contents in the infection sites of mice after being treated with and without ZnPMp (0.5 mg mL^{-1}).

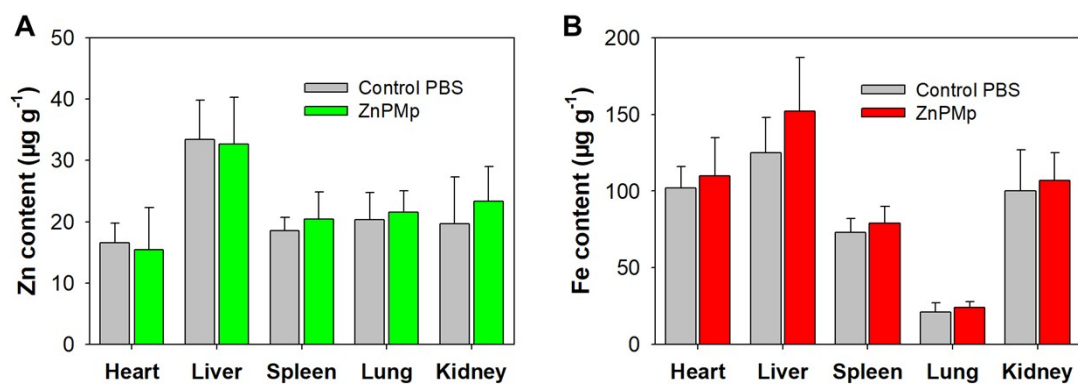


Fig. S19. The *in vivo* biodistribution of Zn (A) and Fe (B) elements in major organs (including heart, liver, spleen, lung and kidney) of mice after being subcutaneously injected with ZnPMp (0.5 mg mL⁻¹) for 14 days.

Supplementary Tables

Table S1. Physiochemical properties of ZnO@Fe/PDA with different amounts of DA added.

Samples	Added DA (%, w/w)	Capped PDA (%, w/w)	Size (nm) ^a	PDI ^b	Zeta potential (mV)	The thickness of PDA (nm)
ZnO	0	0	44.1 ± 11.4	0.14	-14.2 ± 3.5	0
ZnO@Fe/PDA1	1	0.9	45.7 ± 13.4	0.21	-19.4 ± 2.8	1.6 ± 0.6
ZnO@Fe/PDA2	5	4.1	49.8 ± 16.1	0.18	-24.3 ± 4.7	5.7 ± 2.1
ZnO@Fe/PDA3	10	6.7	54.3 ± 14.8	0.24	-29.7 ± 5.3	10.2 ± 3.6

^aDetermined by dynamic light scattering (DLS). ^bPDI, polydispersity index.

Table S2. Sample identifications.

Samples	Description
ZnO@Fe/PDA1	Fe/PDA-capped ZnO nanoparticles (added 1% PDA)
ZnO@Fe/PDA2 (ZnP)	Fe/PDA-capped ZnO nanoparticles (added 5% PDA)
ZnO@Fe/PDA3	Fe/PDA-capped ZnO nanoparticles (added 10% PDA)
ZnPp	PEG-modified ZnO@Fe/PDA2 (ZnP)
ZnPM	MB-loaded ZnO@Fe/PDA2
ZnPMP	PEG-modified and MB-loaded ZnO@Fe/PDA2
PDA-MB	MB-loaded PDA nanoparticles